Baral and Shahandashti
J Infrastruct Preserv Resil (2022) 3:12
https://doi.org/10.1186/s43065-022-00057-2

Journal of Infrastructure Preservation and Resilience

RESEARCH Open Access

Risk-averse rehabilitation decision framework for roadside slopes vulnerable to rainfall-induced geohazards

Anil Baral[1,2*] and Mohsen Shahandashti[1]

Abstract

Rainfall-induced slope failures disrupt the traffic and warrant urgent slope repair works. The impact of roadside slope failures can be minimized if slopes are proactively rehabilitated. Nonetheless, transportation agencies are constrained in their budget to rehabilitate a limited number of slope segments due to competing maintenance needs among different transportation assets. Therefore, the transportation agencies should identify the critical slope combination that should be proactively rehabilitated under constraint budgets to lessen the impact on the transportation network during extreme rainfall events. The decision-making approach for slope rehabilitation should also ensure low risk associated with the selected rehabilitation strategy. Current slope-rehabilitation decision models do not consider the risk associated with the rehabilitation strategies in the decision-making process. The objective of this study is to develop a risk-averse stochastic combinatorial optimization to facilitate the selection of slope rehabilitation strategies, which leads to the least expected cost and conditional value at risk (CVaR) for extreme rainfall events. The simulated annealing approach is used to solve the risk-averse combinatorial optimization rehabilitation problem with the objective function that measures the total cost of traffic disruption and slope restoration post-failures. The approach is demonstrated using a transportation network in Lamar County, Texas. Unlike a genetic algorithm-based approach in the literature that yields a single slope rehabilitation strategy, the proposed risk-averse simulated annealing approach identifies rehabilitation strategies along the Pareto efficient frontier facilitating the rehabilitation decisions based on the tradeoff between expected cost and CVaR. For the network in Lamar County, the proposed risk-averse simulated annealing provided a solution in the Pareto front that reduced CVaR by 2.0% compared to the solution obtained from the genetic algorithm-based approach while only increasing the expected cost by 0.8%. The risk-averse optimization approach will aid transportation agencies in determining slope rehabilitation strategies for minimizing the impact of rainfall-induced failures at appropriate risk aversion levels.

Keywords: Rainfall, Slope failure, Combinatorial optimization, Rehabilitation decision

Introduction

Frequent and intense rainfall events, which are becoming increasingly common with climate change, have threatened the stability of roadside slopes that are crucial for the effective functioning of the road transportation system [37]. Failure of roadside slopes reduces the transportation system efficiency by detours, traffic backups, delays, and additional costs in fuel [2, 3]. The transportation agencies must further deal with the financial burden of slope restorations. Each year, highway agencies spend millions of dollars on restoring failed slopes [7]. The impact of rainfall-induced slope failures can be minimized if slopes in threat of rainfall-induced failures are proactively rehabilitated. However, due to competing rehabilitation

*Correspondence: anil.baral@mavs.uta.edu

[1] Department of Civil Engineering, The University of Texas at Arlington, 416 S. Yates St., Arlington, TX 76019, USA
Full list of author information is available at the end of the article

needs among the infrastructure assets (e.g., bridges, pavement, retaining walls), transportation agencies lack sufficient resources to maintain all the critical roadside slopes in a transportation network [23]. Hence, it is necessary to identify, prioritize, and proactively rehabilitate the slope segments with limited resources available for slope maintenance. The proactive rehabilitation should result in the least disruption of traffic and minimize agency costs (i.e., slope restoration costs) after extreme events triggering rainfall-induced failures. To support the proactive rehabilitation decisions, state transportation agencies such as the Minnesota Department of Transportation (MnDOT) and the Texas Department of Transportation (TxDOT) have performed slope stability analyses to determine the slope failure susceptibility level along the highway corridors [13, 31]. However, due to the limited availability of budget, the state's agencies find themselves in a difficult position to determine the suitable combination of slopes that should be proactively rehabilitated for enhancing the resilience of the transportation system. Let us consider a transportation network (Fig. 1) where three slope segments are susceptible to rainfall-induced failures and transportation agencies cannot rehabilitate slope length more than L_{rehab} due to budget constraints. Each slope segment, i, in the network has length, L_i, and failure probability, P_{fi}. The transportation agencies should rehabilitate a combination of slopes (e.g., $[L_1, L_2]$, $[L_1, L_3]$) that should sum to L_{rehab} and lead to the least failure cost during extreme rainfall events. As rainfall-induced slope failures are probabilistic due to the uncertainty associated with soil mechanical parameters (cohesion and internal angle of frictions) and rainfall intensities [27], the distribution of failure costs under any rehabilitation combination is also probabilistic. Hence, in selecting a rehabilitation strategy, it is essential to ensure the expected cost during extreme events is minimized while also limiting the conditional value at risk associated with the rehabilitation strategy.

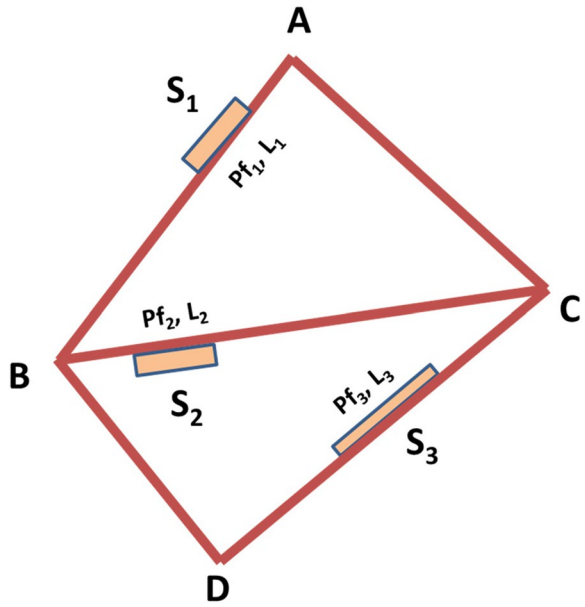

Fig. 1 An example network showing critical slope segments at three locations

Past studies attempted to identify the slope segments with high failure susceptibility along the highway corridors but remain largely silent on how slope rehabilitation should be prioritized under constrained rehabilitation budgets. Hunt [14] prepared a slope failure risk map along transportation corridors based on the assessment of slope geometry, geologic conditions, weather, and surface conditions. The risk maps are solely based on expert judgment, field survey, and interpretation of stereo-pairs of aerial photography. Achour et al. [1] used the Analytic hierarchy process (AHP) and information value (IV) methods to identify the slopes with high failure risk along the highway corridor; the relationship between landslide events and landslide-related factors such as lithology, slope gradient, slope aspect, geotechnical parameter, and distance from fault was carried out in GIS (Geographic Information System) environment. Ramanathan et al. [28] considered six factors (geological formation, slope angle, elevation, slope history, land cover, and precipitation) in the qualitative index overlay method to determine the failure susceptibility of slopes along highway corridors. Pantha et al. [25] used a bivariate statistical model to determine the slope susceptibility indices of roadside slopes and used these indices to prioritize the slope rehabilitation works along the highway corridors. Similarly, Holmstadt et al. [13] used a logistic regression model to assess the failure probability of slopes along the highway corridors in three counties of Minnesota. In addition to the statistical and index-based models, the physics-based models have also been extensively used in assessing roadside slope stability. Mohseni et al. [22] used the infinite slope stability and pore pressure models to determine the rainfall-return periods capable of triggering slope failures along highway corridors. Similarly, Baral et al. [5] used a combination of the hydrological and geotechnical models to identify the rainfall-induced slope failure susceptibility of roadside slopes along highway corridors of Texas. More recently, proactive slope rehabilitation decisions have been determined such that the impact of extreme rainfall events triggering rainfall-induced failures is minimized for both road users and transportation agencies. Baral and Shahandashti [31] developed

a metaheuristic-based optimization approach to identify the most suitable slope rehabilitation strategies for roadside slopes under a constrained rehabilitation budget. The probabilistic slope failure analysis was performed along the highway corridors, and the expected cost of failure was determined for rainfall-induced slope failure scenarios under various rehabilitation strategies. Baral and Shahandashti [31] picked a slope rehabilitation strategy leading to the least cost during extreme rainfall events; however, this study ignores the risk associated with the rehabilitation strategy in the proactive rehabilitation decision-making process. As the slope failures during extreme rainfall events are probabilistic, the cost of failure during extreme rainfall events is also probabilistic. Therefore, the slope rehabilitation strategy should not only minimize the expected cost during catastrophic events but also minimize the conditional value at risk associated with the rehabilitation strategy.

The objective of this research is to identify a combination of roadside slopes that must be proactively rehabilitated with a limited budget to minimize the expected generalized cost E(V) while also limiting the conditional value at risk (CVaR) associated with the rehabilitation strategy. The expected generalized cost E(V) is the average of possible generalized cost (i.e., combined failure cost for user and agency) of different slope failure scenarios under a rehabilitation strategy. The risk of rehabilitation decision is measured as the conditional value at risk (CVaR) associated with a rehabilitation strategy. The CVaR approximates the average of the worst-case generalized costs of the rehabilitation strategy [29, 30]. The rehabilitation strategy with the least CVaR ensures that the risk associated with the rehabilitation decision is low.

Methodology

This section outlines the methodology used for risk-averse simulated annealing to determine the critical slope combination that should be proactively rehabilitated under a constrained budget. The proposed risk-averse simulated annealing approach for the first time incorporates the Conditional Value at Risk (CVaR) borrowed from quantitative finance into a slope rehabilitation decision framework to facilitate the selection of slope segments that should be proactively rehabilitated to minimize expected failure cost and CVaR during extreme rainfall events. Determining the critical roadside slopes combination for proactive rehabilitation involves (1) formulating a risk-averse stochastic combinatorial optimization problem and (2) using a simulated annealing-based approach to solve the stochastic combinatorial optimization problem.

Problem formulation

The optimization problem of minimizing expected generalized cost (V) in a transportation network is defined as:

$$\min_{r\in R_S} E\left(V^r\right) \tag{1}$$

Subjected to

$$\sum_{k=1}^{Ns} n_k C_k \le C_{rehab}$$

$$\mathrm{CVaR}_\alpha \le \mathrm{T}_{\mathrm{cost}}$$

Where R_S represents possible combinatorial space of rehabilitation strategy (r) for proactive maintenance of roadside slopes. Two possible outcomes can be defined for a slope in the generation of a rehabilitation strategy, i.e., either slope can be rehabilitated or left unrehabilitated. For example, consider three slope segments in a road network susceptible to rainfall-induced failure (Fig. 1). The strategy for rehabilitation can be represented as $\{rh_1, rh_2, rh_3\}$, where $rh_i = 0$ represents no rehabilitation, and $rh_i = 1$ represents the rehabilitation of the i^{th} slope segment. Based on this, the possible rehabilitation strategies for network in Fig. 1 are $R_S = \{\{1,1,1\}, \{1,0,1\}, \{0,1,1\}, \{0,0,1\}, \{1,1,0\}, \{1,0,0\}, \{0,1,0\}, \{0,0,0\}\}$. In the absence of constraints, the combinatorial decision space for a transportation network with N number of slope segments requiring repair would be $R_S \in X^{2^N \times N}$. However, the combinatorial decision space is reduced by the optimization constraint that no rehabilitation strategy ($r \in R_S$) can result in a rehabilitation cost that exceeds the available rehabilitation budget (C_{rehab}). The feasible rehabilitation strategy should also have the conditional value at risk less than a specified tolerance cost (T_{cost}).

For the generalized cost (V), which can be represented as a continuous distribution function ($F_X(v)$), $CVaR_\alpha(V)$ is the conditional expectation of V subjected to $V \ge VaR_\alpha(V)$. Figure 2 shows the distribution of generalized costs for a rehabilitation strategy of roadside slopes.

$VaR_\alpha(V)$ represents the value at α-percentile of the random variable V. $CVaR_\alpha(V)$ can be determined using Eq. 2.

$$CVaR_\alpha(V) = \int_{-\infty}^{\infty} v\, dF_X^\alpha(v) \tag{2}$$

Where

$$F_x^\alpha(v) = \begin{cases} 0, & when\ v < VaR_\alpha(V) \\ \frac{F_X(v)-\alpha}{1-\alpha}, & when\ v > VaR_\alpha(V) \end{cases} \tag{3}$$

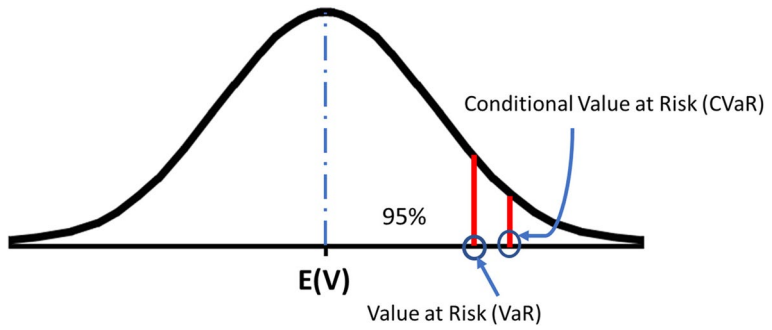

Fig. 2 Generalized cost distribution under a rehabilitation strategy

The distribution parameter N (μ_v, σ_v) of generalized cost (V) for a rehabilitation strategy (r) is determined using the Monte Carlo simulations.

Solving optimization problem

Figure 3 outlines the process used for solving the risk-averse optimization problem. Solving the optimization problem starts with determining slope failure probabilities of roadside slopes. The failure probability of roadside slope is assessed using a combination of physics-based hydrological and geotechnical models incorporating the uncertainty associated with soil cohesion, internal angle of friction, and rainfall intensity [4, 42]. First, the increase in soil water pressure due to rainfall infiltration is determined using the pore pressure response model [16]. Then, the decrease in factor of safety (FOS) due to increased soil water pressure is determined using the infinite slope stability model [34]. The FOS is obtained using Eq. 4.

$$FOS = \frac{tan\phi}{tan\alpha} + \frac{C}{\gamma_s\, z\, sin\alpha.cos\alpha} - \frac{\Psi(\gamma_w)tan\phi}{\gamma_s\, z\, sin\alpha.cos\alpha} \quad (4)$$

where z is the failure depth, α is the slope angle, ϕ is drained fully softened internal angle of friction c is the cohesion, γ_s is the unit weight of soil, γ_w is the unit weight of water, and Ψ is the soil water pressure at failure depth.

In calculating FOS for different landscape pixels, the uncertainty associated with the soil parameters leads to an uncertain forecast of slope stability for roadside slopes. The uncertainty of soil mechanical parameters like internal angle of friction and cohesion is described using the probability density functions [27]. Uniform distribution is desirable to define soil properties in an area where an appropriate range can be specified for soil mechanical properties [42]. The uniform probability distributions for the internal angle of friction and soil cohesion are defined in the range of U (ϕ_{min}, ϕ_{max}) and U (c_{min}, c_{max}). The FOS is determined using Monte Carlo runs for 1000 different generations of frictional angle and cohesion. The probability of slope failure is defined as the ratio of times the FOS is less than 1 to the total number of Monte Carlo runs [27].

Following the determination of slope failure probabilities of roadside slopes, an initial rehabilitation strategy satisfying the cost constraint is generated. For the initial rehabilitation strategy, expected cost and conditional value at risk are determined using the process outlined in Fig. 4.

First, a random number is generated ($R_n \in [0,1]$) and compared with the slope failure probability in a transportation network. If the slope is not repaired based on the current rehabilitation strategy (r) and the failure probability is less than the randomly generated number, disruption is created in the network by blocking the adjacent link. Then, a traffic simulation is performed for the disrupted network, and an increase in user cost due to rerouting is calculated. The user cost includes both the cost associated with delays and additional costs for the operation of vehicles. The agency cost for restoring the failed slopes is also calculated. The generalized cost (i.e., combined user and agency cost) for a rehabilitation strategy $r \in R_S$, is obtained using Eq. 5.

$$V = \sum_i \sum_j d_{ij}^t \left[\Delta T_{ij}^r C_d + \Delta L_{ij}^r C_{op}\right] + C_{sr}^r\Big) \quad (5)$$

where V represents combined user and agency cost for a single run of Monte Carlo simulation when slopes are rehabilitated using a strategy r, d_{ij}^t is the travel demand from node i to node j for the duration of disruption (t), ΔT_{ij}^r is the increase in time traveling from node i to node j and ΔL_{ij}^r is the increase in travel distance from node i to node j, C_d is the cost due to delay and C_{op} is the per mileage cost of maintaining and operating a motor vehicle, and C_{sr}^r is the cost of restoring failed slopes after an extreme rainfall event. The delay cost (C_d) due to traffic disruption is assumed at 30.12 dollars per hour [40], and

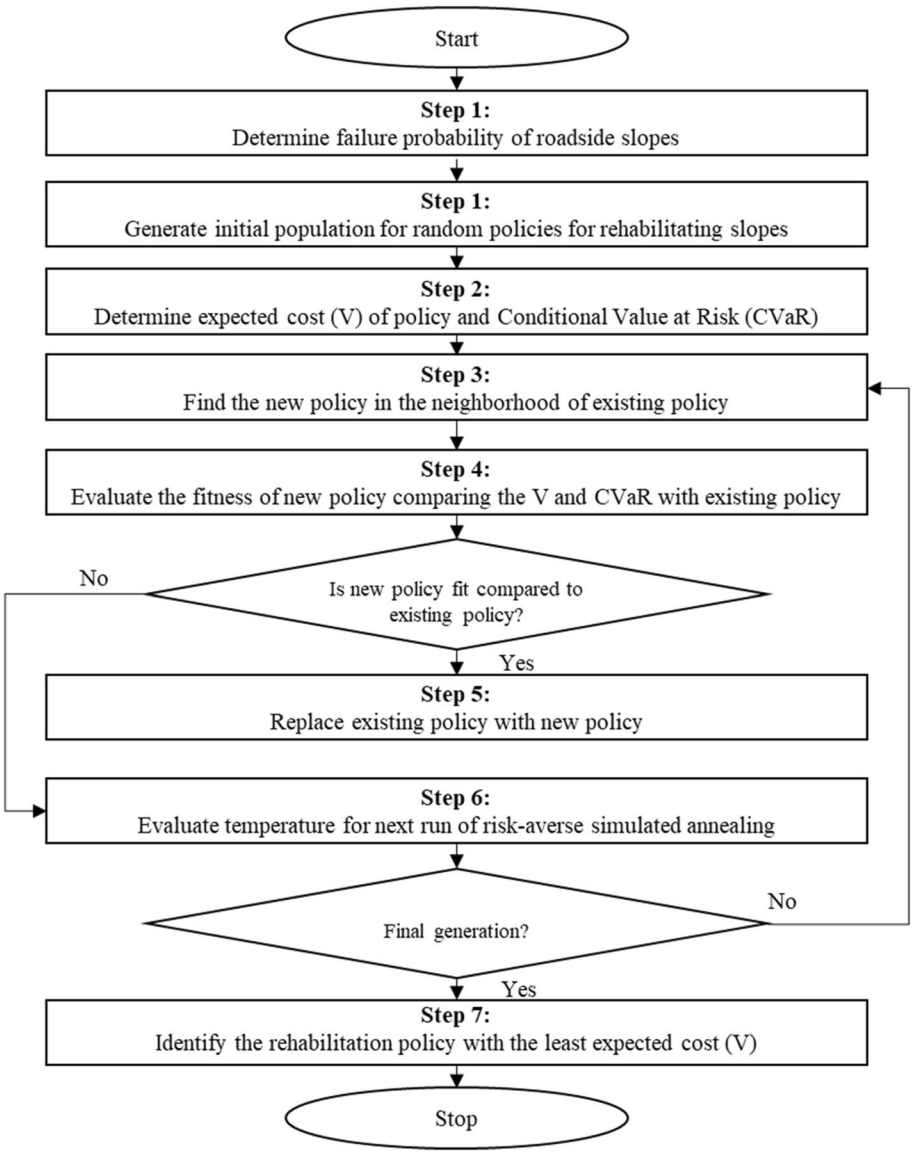

Fig. 3 Steps in the risk-averse simulated annealing process

the cost of operating (C_{op}) a passenger vehicle per mileage is assumed at 67 cents [6]. The traffic disruption is considered one-quarter of a day as this duration was assumed to be adequate to remove the debris caused by shallow slides triggered by rainfalls. The slope restoration cost $\left(C_{sr}^{r}\right)$ is estimated based on the rebuilding and compaction method [31].

After completing N Monte Carlo runs for a rehabilitation strategy r, the list of generalized costs is obtained: $V_i = [V_1, V_2, V_3, \ldots\ldots\ldots V_N]$. The V_i represents N different possible values of generalized cost under a rehabilitation strategy. This distribution of V_i is used to determine the expected value of generalized cost (E(Vr)) and the conditional value of risk $CVaR_{\alpha}(V_r)$ for the rehabilitation strategy r.

The approach outlined in Fig. 4 for calculating expected generalized cost and conditional value at risk is integrated into a risk-averse simulated annealing algorithm to determine the rehabilitation strategy that would lead to the least expected cost while also reducing the conditional value at risk. Due to the probabilistic nature of slope failures, the generalized cost (V) associated with rehabilitation strategies is also stochastic, i.e., generalized cost (V) associated with the rehabilitation strategy follows a probability distribution and can only be analyzed statistically. The inclusion of risk-aversion in the

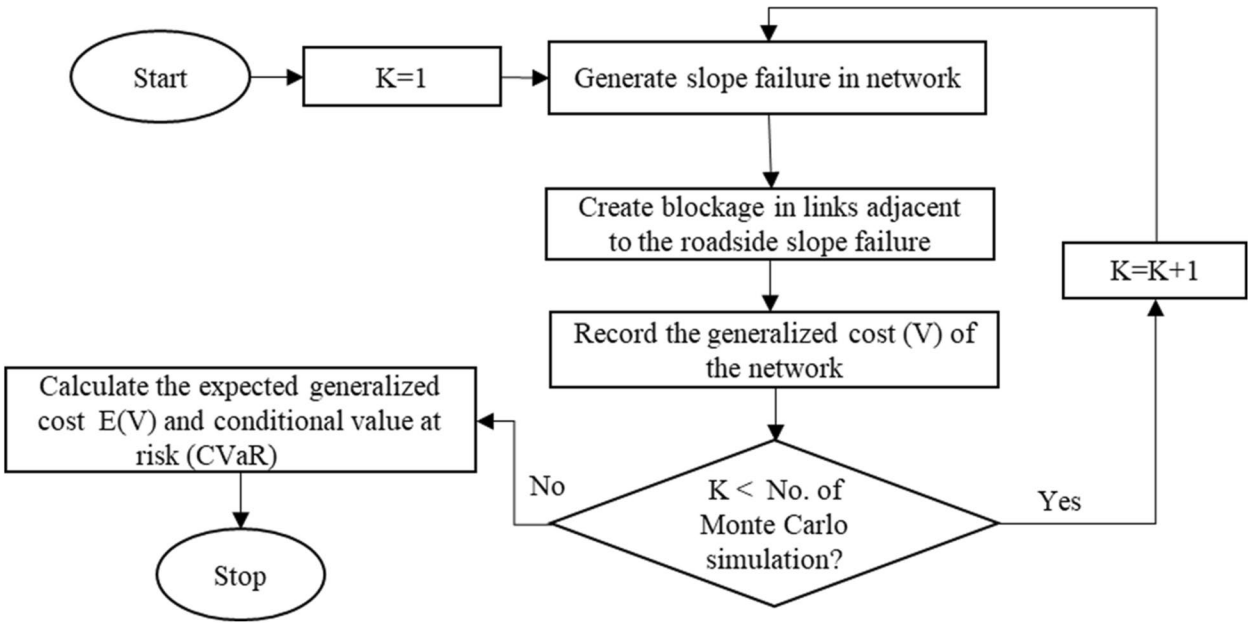

Fig. 4 Calculation of expected cost and conditional value at risk

optimization process enables the selection of rehabilitation strategy considering the tradeoff between expected generalized cost and Conditional Value at Risk (CVaR). Further due to the combinatorial nature of selection of slope segments and the stochastic nature of generalized cost (V), the optimization problem represented by Eq. 1 is a stochastic combinatorial optimization problem. Since Eq. 1 lacks a closed-form representation, a risk-averse simulated annealing approach has been used to determine the rehabilitation strategy that would lead to minimum expected cost at acceptable risk levels. The simulated annealing mimics a solid annealing process, where the state of the solid resembles the possible solutions, energy resembles the objective function of an optimization problem, and the cooling rate of the solid is analogous to a finite sequence of temperature in simulated annealing [19]. The metropolis criterion is used to determine the acceptance or rejection of a new solution at different temperatures during the progression of simulated annealing [21]. At each temperature, mutation of the existing rehabilitation strategy is performed to generate new solutions. At the initial stage of the simulated annealing process, the temperature is set high, thereby increasing the probability of accepting the inferior solutions. With the decrease in temperature, the probability of accepting an inferior solution is decreased and fine-tuning of the optimal solution takes place in the most promising decision space. The time required for converging to an optimal solution is dependent upon the cooling rate and initial temperature. Typically, the initial temperature, cooling rate, and stopping criteria is determined using sensitivity analysis [33].

Following the determination of expected cost (E(Vr)) and conditional value of risk ($CVaR_{\alpha}(V_r)$) of a randomly generated initial rehabilitation strategy (Fig. 3), a new rehabilitation strategy is generated by randomly mutating the 25 % of the binary strings of the old rehabilitation strategy. The initial temperature is set to the generalized cost of failure when no rehabilitation is performed in a network. The fitness of the new rehabilitation strategy is evaluated based on E(Vr) and $CVaR_{\alpha}(V_r)$ of new and existing rehabilitation strategies in each generation of simulated annealing, until the final temperature is reached. The decision of adopting a new rehabilitation strategy compared to the existing rehabilitation strategy (i.e., the old strategy) is based on the following conditions:

Case 1: $\boldsymbol{E(V)_{new} \leq E(V)_{old}}$

Subcase 1a: If the CVaR of the new strategy is less than the old strategy, and the CVaR of the new strategy is also less than the tolerance cost, then the new strategy replaces the old strategy in the next generation of simulated annealing.

Subcase 1b: If the CVaR of the new strategy is more than the previous strategy, then the metropolis function is used to select the rehabilitation strategy for the next generation. A random number ($\lambda \in [0,1]$) is generated and compared with the state of energy Δ given by Eq. 6.

$$\Delta = \exp\left(\frac{-\left(\mathrm{CvaR}_{95}(\mathrm{old})\right) - \left(\mathrm{CvaR}_{95}(\mathrm{new})\right)}{\mathrm{Temp}}\right) \quad (6)$$

Where 'Temp' is the temperature at the current simulated annealing run. The old strategy is replaced by the new when $\lambda < \Delta$. Otherwise, the old rehabilitation strategy is carried to the next generation.

Case 2: $E(V)_{new} > E(V)_{old}$

Subcase 2a: If the generalized cost of the new strategy is greater than the old strategy, but the CVaR of the new strategy is less than the tolerance cost, the state of energy (D) given by Eq. 7 is checked with the randomly generated number ($\beta \in [0,1]$).

$$D = \exp\left(\frac{-(\mathrm{E}(\mathrm{V_{old}})) - (\mathrm{E}(\mathrm{V_{new}}))}{\mathrm{Temp}}\right) \quad (7)$$

Where 'Temp' is the temperature at the current simulated annealing run. The old strategy is replaced by new when $\beta < D$, otherwise old strategy is carried to the next generation.

Subcase 2b: If the generalized cost of the new strategy is greater than the old strategy and the CVaR of the new strategy is also greater than the previous strategy, the state of energy Δ and D are determined as per Eqs. 6 and 7. The old strategy is replaced by new when $\lambda < \Delta$ and $\beta < D$, otherwise the old strategy is carried to the next generation.

Application

The proposed risk-averse optimization approach is used to identify the most suitable slope combination for proactive repair in Loop 286 in Lamar County, Texas. The Loop 286 selected to demonstrate the proposed risk-averse optimization approach is shown in Fig. 5.

First, the slope failure probabilities of slopes along the highway corridors were determined using a combination of the infinite slope stability model [34] and the rainfall infiltration model [16]. This study considered a rainfall of 3-day and a 10-year return period to assess the failure probability of the roadside slopes along the highway corridors [12]. The data on rainfall for the study area is obtained from the Precipitation Frequency Data Server (PDFS), which is operated and maintained National Weather Service (NWS) [24]. A rainfall distribution function for a 3-day duration and 10-year return period in the study region is given by Eq. 8, where g(r) represents the probability of rainfall intensity r. The mean rainfall intensity in the study area is 7.21 in.

$$\mathrm{g(r)} = \frac{1}{0.125\mathrm{x}\sqrt{2\pi}} \exp\left(-\frac{\left(\ln\left(\mathrm{r}/7.21\right)\right)^2}{0.03125}\right) \quad (8)$$

The infinite slope stability and rainfall infiltration models require slope angles and soil properties to determine the slope failure probabilities along the highway corridors. The LiDAR (Light Detection and Ranging)

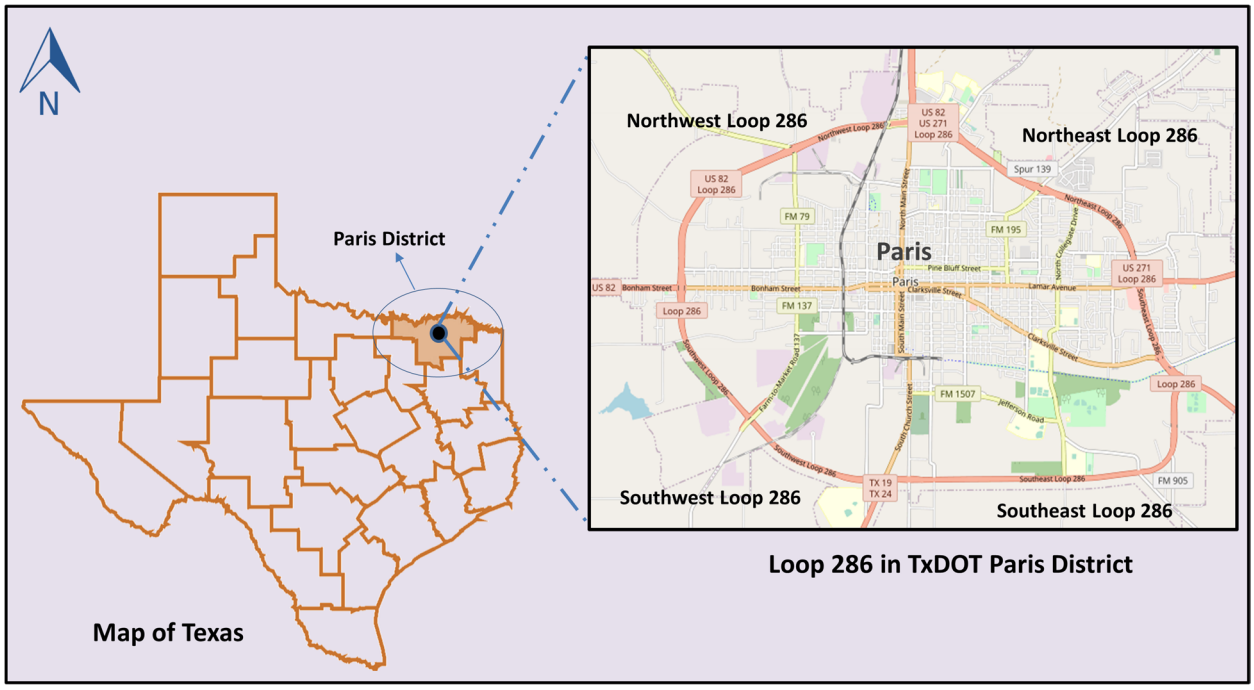

Fig. 5 Loop 286 in the TxDOT Paris district

data was used to determine the slope angles of the landscape. The LiDAR dataset is publicly available by Texas Natural Resource Information System [38]. The LiDAR data was processed in GIS to obtain a slope angle raster with a cell size of 3 m. The soil properties for slopes were obtained from the Soil Survey Geographic (SSURGO) database [35]. The SSURGO database is publicly available by Natural Resource Conservation System (NRCS). Slopes in Lamar County are primarily clayey soils with high shrinkage and swelling potential [32], and slope failures usually occur at fully softened strength [18]. At fully softened strength, the shear strength of soil is considerably reduced, and the cohesion of soil is negligible [17]. Hence, based on past slope failure literature, the cohesion of 50 psf was assumed for calculating slope failure probability [18, 36, 41]. The mean frictional angle for each landscape cell was obtained using the empirical correlation that establishes the relation of frictional angle with Liquid Limit (LL) for different clay fractions and effective stress [11]. After defining the mean cohesion and fully softened frictional angle for each landscape cell, the lower and upper limit of cohesion and friction angle were assumed to lie within 50% of the mean value for developing a probabilistic slope failure map [4, 27]. The cohesion for each pixel was assumed to be in the range of $[0.5 \times c_{\text{mean}}, 1.5 \times c_{\text{mean}}]$, and the internal angle of friction was assumed to be in the range of $[0.5 \times \phi_{\text{mean}}, 1.5 \times \phi_{\text{mean}}]$. After determining the range of values for frictional angle and cohesion, the slope failure probability was determined using a combination of the infinite slope stability model and hydrological model [4]. From the probabilistic slope failure analysis, twenty-one slope segments along the highway corridors were found to have a failure probability greater than 0.2. Park et al. [26] and Ko Ko et al. [20] considered slope failure probability greater than 0.1 and 0.2, respectively, susceptible to slope failures. This study used a failure probability of 0.2 as a cut-off value for narrowing the number of slope segments to be incorporated into the rehabilitation decision framework. Figure 6 shows the twenty-one slope segments considered in the proactive slope rehabilitation framework to demonstrate the risk-averse optimization approach proposed in this study.

For all the 21 slope segments identified to have high failure susceptibility, the slope rehabilitation cost was estimated using the rebuilding and compaction method [31]. For this study, the cost of restoring the slope after failure is assumed to be the same as the cost of proactively rehabilitating the slope segments. The cost of proactively rehabilitating the slope segments is shown in Table 1.

The traffic count data in 98 different locations of the network was obtained from the traffic count database [39]. The open-source simulation package SUMO (Simulation of Urban Mobility) was used to develop the traffic simulation in the network. The OpenStreetMap (OSM)

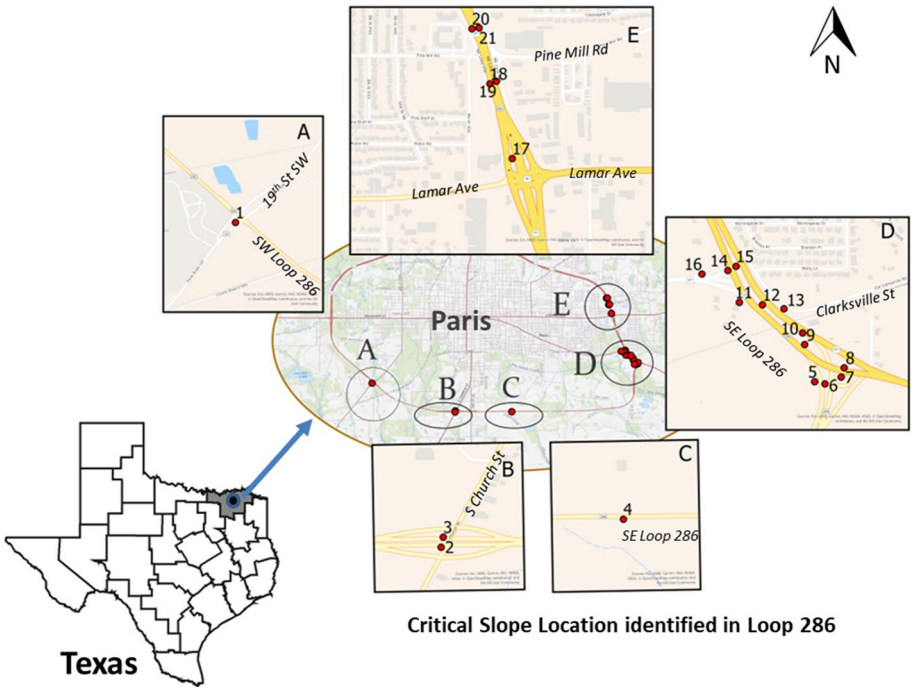

Fig. 6 Slopes with high failure susceptibility in Loop 286 of Paris district, Texas

Table 1 Cost for rehabilitation/restoration of different slope segments

No.	Segment	Failure Probability (P_f)	Longitude	Latitude	Cost of Slope Rehabilitation (USD)
1	*S1*	0.20	−95.58627	33.640225	26,890
2	*S2*	0.42	−95.55988	33.631041	75,574
3	*S3*	0.33	−95.5598	33.631421	50,542
4	*S4*	0.20	−95.54185	33.631145	150,104
5	*S5*	0.28	−95.50286	33.646242	53,022
6	*S6*	0.31	−95.50248	33.646162	74,904
7	*S7*	0.33	−95.50187	33.646415	32,054
8	*S8*	0.41	−95.50176	33.646768	26,132
9	*S9*	0.32	−95.50324	33.647626	88,389
10	*S10*	0.34	−95.50331	33.648061	32,889
11	*S11*	0.33	−95.50568	33.649207	103,890
12	*S12*	0.47	−95.50482	33.649117	83,582
13	*S13*	0.35	−95.50401	33.648972	96,023
14	*S14*	0.27	−95.50611	33.650401	26,142
15	*S15*	0.24	−95.50581	33.650558	58,700
16	*S16*	0.21	−95.50708	33.65027	19,023
17	*S17*	0.21	−95.51022	33.662315	25,721
18	*S18*	0.79	−95.51106	33.665119	18,953
19	*S19*	0.68	−95.51082	33.665211	21,151
20	*S20*	0.81	−95.51173	33.667181	23,787
21	*S21*	0.84	−95.51146	33.667214	23,517
Total Budget Required for Proactive Rehabilitation					**1,110,989**

was used to extract the map of the study area, and a network compatible for running traffic simulation was obtained using the NETCONVERT tool in SUMO [8]. A NETEDIT tool in SUMO was used to manually modify the network [10]. The NETEDIT enables the addition of missing edges, links, connections, and traffic lights in the SUMO network. After the generation of the network, the 'routeSampler' tool was used to heuristically sample routes that matched the traffic count data obtained from the detectors at different locations of the network [9].

After determining all critical slope segments and generation of network traffic, a convergence study was conducted to determine the average number of runs required for convergence of expected cost in each rehabilitation strategy. Figure 7 shows the average generalized cost for different Monte Carlo runs when no slopes in the network are rehabilitated. The convergence study considered no rehabilitation because the uncertainty is highest in the unrehabilitated network compared to a rehabilitated network.

After determining the required number of Monte Carlo runs from the convergence study, a risk-averse simulated annealing approach was used to determine the best slope

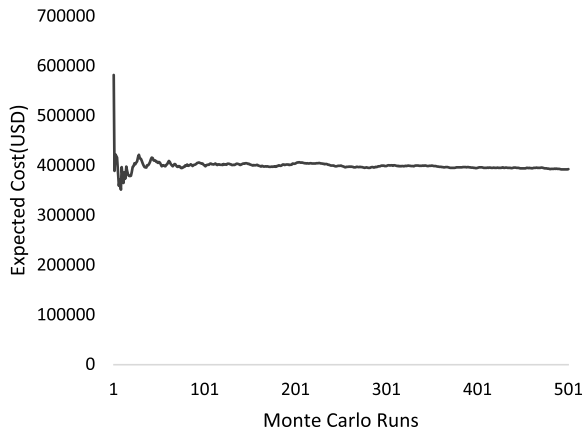

Fig. 7 Convergence study to determine Monte Carlo runs

rehabilitation strategy such that no rehabilitation strategy exceeds 25% of the total rehabilitation budget obtained in Table 1. Also, no rehabilitation strategy can have a conditional value at risk greater than 0.5 million USD. Parameters for risk-averse simulated annealing are shown in Table 2.

The initial temperature in the first run of simulated annealing was set to the expected cost of slope failure considering no rehabilitation of roadside slopes (Fig. 7). Ten iterations were conducted on each temperature. The cooling factor (Table 2) was used to lower the existing temperature after ten iterations of risk-averse simulated annealing. The expected cost and conditional value at risk obtained for different rehabilitation strategies during the progression of risk-averse simulated annealing are shown in Fig. 8. Five rehabilitation strategies (RS1, RS2, RS3, RS4, and RS5) shown in Fig. 8 represent the set of non-dominated solutions. A non-dominated solution set in a multi-objective optimization problem is the list of solutions in which one objective cannot be improved without compromising the other objective [15]. The five rehabilitation strategies RS1, RS2, RS3, RS4, and RS5 shown in Fig. 8 had either expected cost or conditional

Table 2 Parameters for risk-averse simulated annealing

Parameter	Value
Initial Temperature	Expected cost when no slope is rehabilitated
Cooling factor	1.5^{-1}
Final Temperature	Initial Temperature $\times 1.5^{-30}$
Iteration per temperature	10
Monte Carlo runs for Convergence	250
Total iteration for Simulated Annealing	300

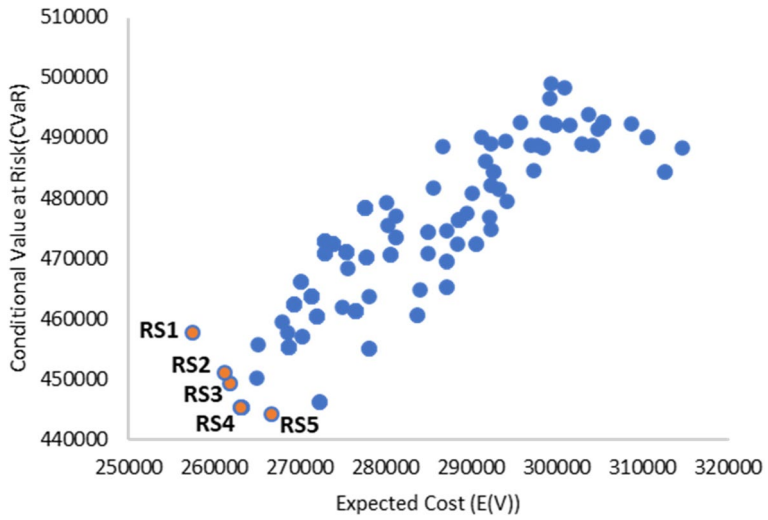

Fig. 8 Expected cost and Conditional Value at Risk for different rehabilitation policies obtained during the progression of simulated annealing

value at risk lower than the other policies. The rehabilitation strategies represented by RS1, RS2, RS3, RS4, and RS5 are shown in Table 3. The rehabilitation strategies RS1, RS2, RS3, RS4, and RS5 recommended the strategies for which the rehabilitation cost was 23.40, 24.24, 24.71, 23.26, and 23.86% of the rehabilitation budget obtained in Table 1. The non-dominated solutions obtained from the proposed risk-averse simulated annealing help transportation agencies select the optimum rehabilitation strategies with different risk-aversion levels.

Table 3 Slopes rehabilitated under strategies RS1, RS2, RS3, RS4, and RS5

S.N.	Segment	Rehabilitation Strategy				
		RS1	RS2	RS3	RS4	RS5
1	*S1*	0	0	0	0	0
2	*S2*	0	0	0	0	1
3	*S3*	0	0	0	0	0
4	*S4*	0	0	0	0	0
5	*S5*	0	0	0	1	0
6	*S6*	1	0	0	0	0
7	*S7*	0	0	1	1	0
8	*S8*	1	1	1	1	0
9	*S9*	0	0	0	0	0
10	*S10*	1	0	1	0	0
11	*S11*	0	0	0	0	0
12	*S12*	1	1	0	1	1
13	*S13*	0	1	1	0	0
14	*S14*	0	0	0	0	0
15	*S15*	0	0	0	0	1
16	*S16*	0	0	0	0	0
17	*S17*	0	0	0	0	0
18	*S18*	1	1	1	1	0
19	*S19*	0	1	1	1	0
20	*S20*	0	0	1	0	1
21	*S21*	1	1	1	1	1

Note: 1 represents rehabilitation and 0 represents no rehabilitation of the slope segment

Validation

The proposed risk-averse optimization approach was compared with the approach proposed by Baral and Shahandashti [31], who used a genetic algorithm-based optimization approach to identify the critical combination of roadside slopes for proactive rehabilitation. This genetic algorithm-based approach for identifying the slope rehabilitation strategy was shown to outperform the existing index-based approach for prioritizing slope rehabilitation works [5]. As the genetic algorithm-based optimization approach ignored the conditional value at risk (CVaR) associated with rehabilitation strategy, the importance of considering the risk-aversion in the optimization framework could be easily illustrated when the genetic algorithm-based approach was compared with the risk-averse simulated annealing approach proposed in this study. Initially, five random policies were generated such that no rehabilitation strategy exceeded 25% of the total rehabilitation budget obtained in Table 1. The expected costs of the randomly generated five policies were determined and a two-point cross-over was performed on the rehabilitation policies with the least expected cost during each progression of genetic algorithms. The genetic algorithm was performed for 100 generations. The mutation was performed for 20% of the bits in the rehabilitation strategy. The initial mutation rate was 90% and was gradually decreased by 5% in each generation of the genetic algorithm.

Figure 9 shows the expected cost and CVaR of rehabilitation strategies obtained from the risk-averse simulated annealing and the genetic algorithm-based rehabilitation optimization approach that neglects the consideration of risk aversion in the optimization process. The genetic algorithm-based approach recommended the rehabilitation of slope segments S2, S3, S12, S18, S19, and S21. The genetic algorithm-based approach provides a single solution in the Pareto efficient frontier (Fig. 9) limiting the choice of slope rehabilitation for the decision-makers. On the other hand, the proposed risk-averse simulated annealing approach provide decision-makers a range of solution in the risk-return space with different expected cost and CVaR. Compared to the CVaR of rehabilitation strategy GA-RS obtained from the genetic algorithm-based approach (Fig. 9), the CVaR of the rehabilitation strategy RS4 identified by the proposed risk-averse simulated annealing approach is lower by 2%. On the other hand, the expected cost of rehabilitation strategy RS4 is only higher by 0.8% compared to the expected cost of rehabilitation strategy GA-RS (Fig. 9). Hence, the proposed risk-averse simulated annealing approach helps in the selection of rehabilitation strategy of slope considering the suitable tradeoff between expected cost and CVaR.

Discussion

The approach to slope management in transportation agencies has so far been reactive. i.e., the slopes are only repaired after rainfall-induced failures disrupt the transportation network. This study provides transportation agencies with a tool to facilitate proactive decision-making. The risk-averse slope rehabilitation decision approach proposed in this study enables the identification

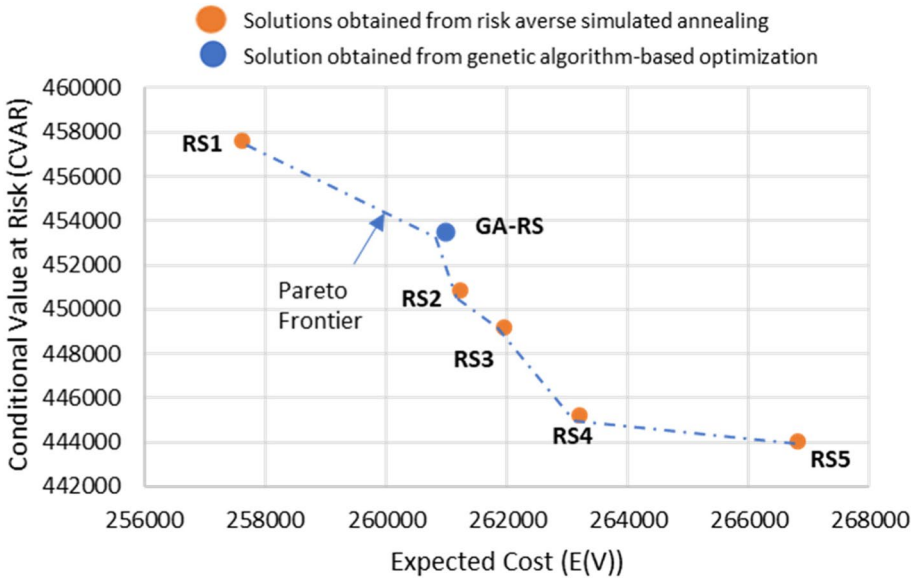

Fig. 9 Comparison of rehabilitation optimization results with and without the risk-averse condition

of the most promising combination of slopes that should be proactively rehabilitated with a limited budget to minimize the impacts of rainfall-induced geohazard on highway networks. While allocating all the resources to respond to rainfall-induced failure in wet seasons can be an effective way to act in response to slope failure, reactive maintenance does not improve the resilience of roadside slopes. Hence, slope management supported by a proactive slope maintenance decision framework is vital to improve the resilience of slopes that are increasingly threatened by extreme rainfall events.

At present, the proposed risk-averse simulated annealing approach considers the impact of rainfall-induced failures on road users and agencies for facilitating proactive rehabilitation decision-making under a constrained rehabilitation budget. The proposed approach does not consider planning time horizon or resilience of repair methods in determining the rehabilitation strategies. However, the approach presented in this research can fit inside the slope management program considering the time horizon. For example, in a 10-year planning horizon, the approach presented in this study helps to identify the most suitable combination of slopes that should be proactively rehabilitated each year with the limited annual maintenance budget. The number of slope segments to be considered each year in the decision framework will depend on the failure probability of the slopes. While determining the failure probability of slopes can be straightforward, the determination of the failure probability of rehabilitated slopes is dependent on the resilience offered by the slope stabilization technique, the quantification of which exceeds the scope of this study. Future studies are required to determine the resilience offered by different repair techniques to support the slope management planning over the time horizon.

Conclusion

A risk-averse combinatorial optimization problem was devised to identify the critical combination of slopes that must be rehabilitated to minimize the impact of rainfall-induced slope failures on the highway networks. The combinatorial optimization problem was solved using a simulated annealing approach. The objective of the combinatorial optimization problem was to minimize the user and agency costs during the extreme rainfall events triggering slope failure. The rehabilitation was constrained by the agency's limitation to rehabilitate only a limited length of slope segment due to budget constraints and with the risk aversion level such that the conditional value at risk does not exceed the tolerance cost. The application of the proposed risk-averse optimization approach was demonstrated using a highway network in the Paris district, Texas. The rehabilitation was constrained so that no strategy can recommend rehabilitation exceeding 25% of the total budget required for proactive maintenance. A set of non-dominated solutions (i.e., rehabilitation strategies) on the Pareto front were obtained at the end of the simulated annealing process. The results were compared with the latest methodology in literature for determining the proactive rehabilitation strategy for roadside slopes. The comparison showed that the proposed risk-averse simulated annealing was able to identify the list of solutions with different risk-aversion levels, thereby diversifying the selection of rehabilitation strategies for the roadside slopes. The proposed approach will help transportation agencies to identify the most suitable combination of slopes for rehabilitation within acceptable risk tolerance levels under a constrained rehabilitation budget.

Acknowledgements
Not Applicable.

Authors' contributions
AB and MS conceived the proposed study. AB collected the data, performed the experiments, and interpreted the results. AB drafted the paper and MS conducted a detailed review of the paper. MS supervised the entire research work. Both authors reviewed the final draft of the paper. The authors read and approved the final manuscript.

Funding
The authors declare that no funds, grants, or other support were received during the preparation of this manuscript.

Availability of data and materials
The datasets used and/or analyzed during the current study are available from the corresponding author on reasonable request.

Declarations

Ethics approval and consent to participate
Not Applicable.

Consent for publication
All authors consent to the publication.

Competing interests
The authors declare that they have no competing interests.

Author details
[1]Department of Civil Engineering, The University of Texas at Arlington, 416 S. Yates St., Arlington, TX 76019, USA. [2]Present Address: Transportation Division, VRX, Inc., 2500 Dallas Pkwy Ste 450, Plano, TX 75093, USA.

Received: 18 June 2022 Revised: 26 July 2022 Accepted: 12 August 2022
Published online: 10 October 2022

References

1. Achour Y, Boumezbeur A, Hadji R, Chouabbi A, Cavaleiro V, Bendaoud EA (2017) Landslide susceptibility mapping using analytic hierarchy process and information value methods along a highway road section in Constantine, Algeria. Arab J Geosci 10(8):1–16
2. Anderson SA, Rivers BS (2013) Corridor management: a means to elevate understanding of geotechnical impacts on system performance. Transp Res Rec 2349(1):9–15

3. Baral A, Shahandashti SM (2022a) A data integration approach for assessment of rainfall-induced slope failure susceptibility. In: *Construction research congress 2022*, pp 480–489
4. Baral A, Shahandashti SM (2022b) Identifying critical combination of roadside slopes susceptible to rainfall-induced failures. Nat Hazards 1-22. https://doi.org/10.1007/s11069-022-05343-6
5. Baral A, Poumand P, Adhikari I, Abediniangerabi B, Shahandashti M (2021) GIS-based data integration approach for rainfall-induced slope failure susceptibility mapping in clayey soils. Nat Hazards Rev 22(3):04021026
6. BTS (Bureau of Transportation Statistics) (2021) Average cost of owning and operating an automobile Available at https://www.bts.dot.gov/content/mile-costs-owning-and-operating-automobile Accessed 20 Mar 2022
7. Collin JG, Loehr JE, Hung CJ (2008) Highway slope maintenance and slide restoration: reference manual (no. FHWA-NHI-08-098) National Highway Institute (US)
8. DLR (German Aerospace Center) (2021) Netconvert - SUMO documentation SUMO. https://sumo.dlr.de/docs/netconvert.html (Accesses 8 Mar 2022)
9. DLR. (German Aerospace Center) German Aerospace Center (DLR) (2021) Routesamplerpy - SUMO documentation SUMO. https://sumo.dlr.de/docs/Tools/Turns.html#routesamplerpy (Accesses 8 Mar 2022)
10. DLR. (German Aerospace Center) (2021) Netedit - SUMO documentation SUMO. https://sumo.dlr.de/docs/netedit.html (Accesses 8 Mar 2022)
11. Gamez JA, Stark TD (2014) Fully softened shear strength at low stresses for levee and embankment design. J Geotech Geoenviron 140(9):06014010
12. GCO (Geotechnical Control Office), Engineering Development Department Hong Kong (1984) Geotechnical manual for slopes Geotechnical Control Office, Public Works Department
13. Holmstadt J, Bradley N, Rodgers N (2020) *Phase 3 MnDOT slope vulnerability assessments* (no. MN 2020-21). Department of Transportation, Minnesota
14. Hunt RE (1992) Slope failure risk mapping for highways: methodology and case history. Transp Res Rec 1343:42–51
15. Hwang CL, Masud ASM (2012) Multiple objective decision making—methods and applications: a state-of-the-art survey (Vol. 164). Springer Science & Business Media
16. Iverson RM (2000) Landslide triggering by rain infiltration. Water Resour Res 36(7):1897–1910
17. Jafari N, Puppala A (2019) Prediction and rehabilitation of highway embankment slope failures in changing climate
18. Kayyal MK, Wright SG (1991) Investigation of long-term strength properties of Paris and Beaumont clays in earth embankments. Final rep. No. FHWA/TX-92+1195-2F. Federal Highway Administration, Washington, DC
19. Kirkpatrick S, Gelatt CD Jr, Vecchi MP (1983) Optimization by simulated annealing. Science 220(4598):671–680
20. Ko Ko C, Flentje P, Chowdhury R (2004) Landslides qualitative hazard and risk assessment method and its reliability. Bull Eng Geol Environ 63(2):149–165
21. Metropolis N, Rosenbluth AW, Rosenbluth MN, Teller AH, Teller E (1953) Equation of state calculations by fast computing machines. J Chem Phys 21(6):1087–1092
22. Mohseni O, Strong M, Grosser AT, Hathaway C, Mielke AM (2017) Mapping slope-failure susceptibility for infrastructure management. In: *Congress on technical advancement 2017*, pp 69–78
23. National Academies of Sciences, Engineering, and Medicine (2019) Geotechnical asset Management for Transportation Agencies, volume 1: research overview. The National Academies Press, Washington, DC. https://doi.org/10.17226/25363
24. NOAA (National Oceanic and Atmospheric Administration) 2018. NWS/Office of Water Prediction, Hydrometeorological Design Studies Center (September 26, 2018). Precipitation Frequency for Texas, USA – NOAA Atlas 14 Volume 11. Retrieved on June 22, 2019, Available at: https://hdsc.nws.noaa.gov/hdsc/pfds/
25. Pantha BR, Yatabe R, Bhandary NP (2010) GIS-based highway maintenance prioritization model: an integrated approach for highway maintenance in Nepal mountains. J Transp Geogr 18(3):426–433
26. Park HJ, Lee JH, Woo IK (2013) Assessment of rainfall-induced shallow landslide susceptibility using a GIS-based probabilistic approach. Eng Geol 161:1–15
27. Raia S, Alvioli M, Rossi M, Baum RL, Godt JW, Guzzetti F (2014) Improving predictive power of physically based rainfall-induced shallow landslide models: a probabilistic approach. Geosci Model Dev 7(2):495–514
28. Ramanathan R, Aydilek AH, Tanyu BF (2015) Development of a GIS-based failure investigation system for highway soil slopes. Front Earth Sci 9(2):165–178
29. Rockafellar RT, Uryasev S (2002) Conditional value-at-risk for general loss distributions. J Bank Financ 26(7):1443–1471
30. Sarykalin S, Serraino G, Uryasev S (2008) Value-at-risk vs. conditional value-at-risk in risk management and optimization. In: *State-of-the-art decision-making tools in the information-intensive age*, pp 270–294 Informs
31. Shahandashti M, Hossain S, Baral A, Adhikari I, Pourmand P, Abediniangerabi B (2022) *Slope repair and maintenance management system* (no. FHWA/TX-20/5-6957-01-1) Texas Department of Transportation
32. Shahandashti M, Hossain S, Zamanian M, Akhtar MA (2021) *Advanced geophysical tools for geotechnical analysis* (no. FHWA/TX-20/0-7008-1) Texas Department of Transportation
33. Shahandashti SM, Pudasaini B (2019) Proactive seismic rehabilitation decision-making for water pipe networks using simulated annealing. Nat Hazards Rev 20(2):04019003
34. Skempton AW, Delory IA (1957) Stability of natural slope in clayey soil. In: Proc., 4th Int. Conf. On soil mechanics and foundation engineering. International Society for Soil Mechanics and Geotechnical Engineering, London
35. Soil Survey Staff (2020). Soil Survey Geographic (SSURGO) Database. Retrieved on June 22, 2020. Natural Resources Conservation Service, United States Department of Agriculture. Available online at: https://sdmdataaccess.sc.egov.usda.gov
36. Stauffer PA, Wright SG (1984) An examination of earth slope failures in Texas. Research rep. Center for Transportation Research, Univ. of Texas, Austin, pp 353–33F
37. Thompson PD, Beckstrand D, Mines A, Vessely M, Stanley D, Benko B (2016) Geotechnical asset management plan: analysis of life-cycle cost and risk. Transp Res Rec 2596(1):36–43
38. TNRIS (Texas Natural Resource Information Center). (2019). Elevation-LiDAR. Retrieved on March 5, 2019. Available at: https://tnris.org/stratmap/elevation-lidar/
39. TxDOT (2021) Traffic count database system (TCDS) Texas Department of Transportation. https://txdot.ms2soft.com/tcds/tsearch.asp?loc=Txdot&mod=TCDS
40. TxDOT (2022) Road user cost Texas Department of Transportation. Available at https://www.txdot.gov/inside-txdot/division/construction/road-user-costs.html
41. Wright SG, Zornberg JG, Aguettant JE (2007) The fully softened shear strength of high plasticity clays (no. FHWA/TX-07/0-5202-3)
42. Zhang S, Zhao L, Delgado-Tellez R, Bao H (2018) A physics-based probabilistic forecasting model for rainfall-induced shallow landslides at regional scale. Nat Hazards Earth Syst Sci 18(3):969–982

Publisher's Note